APPLIED BIOCHEMISTRY AND BIOTECHNOLOGY 6, 37 51 (1981)

Determination of Intrinsic Properties of Immobilized Enzymes

2. Kinetic Studies on Sepharose–Staphylococcal Nuclease in the Presence of Diffusional Limitations

JOSÉ M. GUISÁN, FRANCISCO V. MELO, AND ANTONIO BALLESTEROS*

Instituto de Catálisis y Petroleoquímica, Consejo Superior de Investigaciones Científicas, Madrid, Spain

Received May 21, 1980; Accepted November 21, 1980

Abstract

Using a small substrate (thymidine 5'-(*p*-nitrophenyl phosphate) 3'-phosphate), the kinetics of staphylococcal nuclease insolubilized on CNBr-activated Sepharoses 4B and 6B are affected by internal diffusional limitations. Since we demonstrate that we are working under conditions in which external mass-transfer resistances do not influence the reaction rate, we propose a simple theoretical model that considers only the case of mixed enzymic reaction-internal diffusion kinetics. In the Eadie-Hofstee plots we find very good agreement between theory and experiment. The model accounts very well for the results obtained by changing support texture, reaction conditions, and/or enzyme concentration in the insoluble derivatives, variables that modify the diffusional restrictions of the system.

Index Entries: Sepharose-staphylococcal nuclease; staphylococcal nuclease, immobilized; diffusion effects, on Sepharose-staphylococcal nuclease; kinetics, of Sepharose-staphylococcal nuclease; immobilized staphyococcal nuclease; immobilized enzymes.

Introduction

In the companion paper (*1*) we have studied a simple catalytic system in which the measured kinetic properties are the true intrinsic kinetic properties of the

0273 2289/81/0300 0037$03.00

insolubilized enzyme. Modifications to this basic system provide more complicated systems in which the influence of diffusional, steric, or electrostatic effects can be readily studied. There (*1*) we examined the system formed by insolubilized derivatives of staphylococcal nuclease covalently bound to Sepharose 2B and a model substrate, thymidine 5'-(*p*-nitrophenyl phosphate) 3'-phosphate (NPpdTp). We reasoned that because of the small size of the substrate and the great pore size of the support, diffusional effects were absent and the kinetic constants obtained could be considered the true kinetic constants of the insolubilized nuclease. In the present paper, a detailed study of diffusional effects has been made by extending those studies to nuclease derivatives prepared using as supports Sepharose 4B and Sepharose 6B. The latter differ from Sepharose 2B only in having smaller pore size.

The effect of diffusion in immobilized enzyme systems is very well documented. Theoretical models have been proposed (*2–13*), but the fit of the predicted model to the experimental data has been considered in only a few cases (*8, 11, 13*). On the other hand, and since we are working on the hydrolysis of nucleic acids by these insolubilized nuclease derivatives, the data obtained with the model substrate NPpdTp will constitute important background knowledge towards an understanding of the very complicated kinetic process taking place when these insolubilized nuclease derivatives hydrolize their natural macromolecular substrates.

In this paper we present first a theoretical model accounting for the influence of diffusional limitations on the kinetic behavior of insolubilized enzyme derivatives. Since we have already confirmed (*1*) the absence of external diffusional limitations with the Sepharose 2B–nuclease derivatives, now in the case of Sepharose 4B– and Sepharose 6B–nuclease derivatives, we can also expect external diffusion not to influence the overall rate. This prediction has been confirmed (see Results). In the theoretical model described below we have therefore considered only mixed internal diffusion- and reaction-controlled kinetics.

Experimental results obtained with our system (Sepharose–nuclease as catalyst and NPpdTp as substrate) have been fitted to the theoretical model. In all cases a single procedure is used for the adjustment of experimental and theoretical Eadie—Hofstee plots. In addition, the variation of the diffusional restrictions with changes in the reaction conditions or in the characteristics of the insoluble derivatives has been studied.

Theory

Internal Diffusion-Enzymic Reaction

This limiting case has been very well studied (*2, 3, 5, 9, 11*), using similar mathematical models. We consider an insoluble enzyme system having the following properties: (a) the solid support particles are spherical; (b) the enzyme is uniformly distributed in the porous matrix, the amount of enzyme insolubilized on the external surface being negligible; (c) the flux of substrate

across the porous network follows Fick's law; and (d) the enzymatic reaction (hydrolysis) is monosubstrate. Then, following the reasoning of Marsh (*5*), at steady state the concentration profile for the substrate within a particle containing enzyme is given by (in a dimensionless form):

$$d^2Y/d\rho^2 + (2/\rho)(dY/d\rho) - \theta^2\,\beta\,[Y/(\beta + Y)] = 0 \qquad (1)$$

where

$$Y = S(r)/S_o \qquad \rho = r/R \qquad \beta = K'_M/S_o$$

and

$$\emptyset = R(k'_{cat}E_{gel}/K'_M D_{eff})^{1/2} \qquad (2)$$

The boundary conditions for Eq. (1) are

$$dY/d\rho = 0 \quad \text{at} \quad \rho = 0$$

$$Y = 0 \quad \text{at} \quad \rho = 1$$

One way of calculating the effectiveness factor, η, is to consider that at steady state the actual reaction rate in the whole sphere is equal to the rate of diffusion of the substrate through the entire surface towards the inside of the sphere. Then

$$\eta = \frac{\text{actual overall reaction rate, } S(r) = S(r)}{\text{reaction rate if } S(r) = S_o}$$

$$= 4\,\pi R^2 D_{eff}\,(dS/dr)_{r=R}/\int_0^R 4\,\pi R^2\,[k'_{cat}E_{gel}S_o dr/(K'_M + S_o)] \qquad (3)$$

Integrating Eq. (3) and expressing the solution in dimensionless form, we obtain

$$\eta = [3(\beta + 1)/\emptyset^2\,\beta]\,(dY/d\rho)_{\rho=1} \qquad (4)$$

A computer program using the fourth-order integration method of Runge-Kutta (*14*) was assembled. By solving Eq. (1) numerically, we have calculated the value of $(dY/d\rho)_{\rho=1}$ for different given values of β and $\emptyset$. Thus, we have obtained the function $\eta = f(\emptyset, \beta)$. Our results are very similar to those of Marsh (*5*), who solved η in a different way.

In the limiting cases of Michaelian kinetics defined by $\beta \to 0$ (zero-order) and $\beta \to \infty$ (first-order), the solutions to Eq. (1) are the same as those obtained previously for the general case of porous catalysts (*15, 16*):

Zero order

$$\eta_o = 1 \text{ when } \emptyset \leqslant (6/\beta)^{1/2}$$

$$\eta_o = 1 - \rho_e^3 \text{ when } \emptyset > (6/\beta)^{1/2}$$

where ρ_e is defined by

$$\emptyset^2\beta = 3/(1 - \rho_e)\,[1/2\,(1 + \rho_e) - \rho_e^2]$$

Then $\eta_o = f(\emptyset, \beta)$

First order

$$\eta_1 = (3/\emptyset)\,[(1/\tanh\,\emptyset) - (1/\emptyset)] \tag{5}$$

Then $\eta_1 = f(\emptyset)$

In general, the actual overall reaction rate in a particle of insoluble derivative will be

$$v_p = \eta\,(\emptyset, \beta)\; k'_{cat} E_{gel} S_o/(K'_M + S_o) \tag{6}$$

In the absence of internal diffusional limitations, $\eta = 1$ and this equation coincides with Eq. (1) of the preceding paper (*1*).

From this simple presentation follows the basis of the test carried out in the preceding paper (*1*) to check for the existence of internal diffusion limitations. We can write the following expressions:

$$v_p = f[\emptyset(R)] \text{ if } \eta < 1$$

and

$$v_p \neq f[\emptyset(R)] \text{ if } \eta = 1$$

$$v_p/E_{gel} = f[\emptyset(E_{gel}^{1/2})] \text{ if } \eta < 1$$

and

$$v_p/E_{gel} \neq f[\emptyset(E_{gel}^{1/2})] \text{ if } \eta = 1$$

This means that internal diffusion restrictions will not control the process if the reaction velocity is independent of the size of the particles and if it is also directly proportional to E_{gel}.

Rate of Product Appearance in a Stirred Batch Reactor

Following the reasoning of the preceding paper (*1*), we have

$$v_p = v_R/\gamma = \eta\,(\emptyset, \beta)\,[k'_{cat}\; E_{gel}\; S_o/(K'_M + S_o)] \tag{7}$$

In order to analyze the experimental data we have chosen the Eadie-Hofstee type of plot, which is, for several reasons, particularly useful for the analysis of the influence of diffusion on the kinetic behavior of insolubilized enzymes. (a) In general, this plot is the most suitable for detecting any deviation from the linearity typical of Michaelis-Menten kinetics, as has been suggested and analyzed by Dowd and Riggs (*17*). (b) In this plot the approximations to zero- and first-order kinetics are readily obtained by extrapolation to the abscissa and ordinate axes, respectively. These approximations, which become very important for the analysis of diffusional limitations, were used earlier by Kasche et al. (*2*) and will be employed in the present study for the adjustment of the experimental data to the theoretical model. With the other two plots classical in enzyme kinetics, only one of those approximations is obtained by extrapolation, whereas the other must be obtained as an asymptotic limit. (c) Mixed internal diffusion–enzymic reaction kinetics yield sigmoidal curves in the Eadie-Hofstee representation, whereas if additional external diffusion restrictions are present the sigmoidal curves will then show a downward

concavity pattern. On the other hand, the limiting case of mixed external diffusion–enzymic reaction, more likely to be encountered if the enzyme is insolubilized on nonporous supports, produces a concave graph, as has been discussed by Engasser and Horvath (*18*).

For the Eadie-Hofstee analysis, Eq. (7) can be transformed into

$$(v_R/\gamma)/E_{gel}S_o = \eta\ (\emptyset, \beta)\ [(k'_{cat}/K'_M) - (1/K'_M)\ (v_R/\nu/E_{gel})] \qquad (8)$$

In this representation the points corresponding to each β value are on a straight line going through the origin and whose slope is β/K'_M.

Depending on the values of $\emptyset$ and β we will obtain different types of representation:

(i) Enzymic kinetics: When $\emptyset$ takes a value such that $\eta = 1$ for all β values, then the enzymic reaction controls the overall rate. Equation (8) becomes Eq. (3) of the preceding paper (*1*).

(ii) Internal diffusion kinetics: When for every value of β, $\eta = f(\emptyset, \beta) < 1$, Eadie-Hofstee plots will not follow a straight line, since η varies with β (and, consequently, with S_o). However, if $\beta \to \infty$, the points will fit a straight line of equation

$$(v_R/\gamma)/E_{gel}S_o = \eta_1\ (\emptyset)\ [(k'_{cat}/K'_M) - (1/K'_M)\ (v_R/\nu/E_{gel})] \qquad (9)$$

(iii) Mixed internal diffusion-enzymic reaction kinetics: This case applies when the value of the Thiele modulus is such that $\eta = 1$ for certain (low) values of β, whereas $\eta = f(\theta, \beta) < 1$ for low substrate concentrations. For $\beta \to \infty$, the curve tends to follow Eq. (9). Thus, in mixed kinetics we will observe the sigmoidal pattern.

Figure 1 shows the theoretical Hofstee plots of three insolubilized enzyme derivatives having different Thiele moduli as compared with the straight line corresponding to the soluble enzyme (Michaelian kinetics). For the entire range of β ($0 < \beta < \infty$) all the representations belong to type(iii). Usually β can not be varied experimentally throughout all that range; if however we consider only the region $0.1 < \beta < 2$ (see Fig. 1), then the representation is of type(i) for $\emptyset = 1.3$, of type (ii) for $\emptyset = 7$, and of type(iii) (mixed internal diffusion–enzymic reaction kinetics) for $\emptyset = 3.6$.

The fitting of the experimental data to the theoretical model is easy when k'_{cat} and K'_M are known. One has only to extrapolate the experimental points to the ordinate axis bearing in mind that the last part of the curve must tend to be a straight line parallel to the one corresponding to enzymic kinetics. The intersection point will be $\eta_1\ (\emptyset)\ k'_{cat}/K'_M$ and once η_1 is known we can calculate $\emptyset$ by Eq. (5). Then the theoretical curve for such a value of $\emptyset$ is compared with the experimental data in order to achieve the best possible fitting. This may require several extrapolations to the ordinate axis.

When owing to the characteristics of the insoluble derivatives and/or of the reaction itself, the diffusional restrictions are important, then it is not possible to obtain k'_{cat} and K'_M experimentally. In this case it will be necessary to have as many data as possible at very high values of β, so that we have to extrapolate only a small region of the graph. We will need for our calculations not only the intersection at the ordinate ($= \eta_1 k+_{cat}/K'_M$), but also the slope of that last

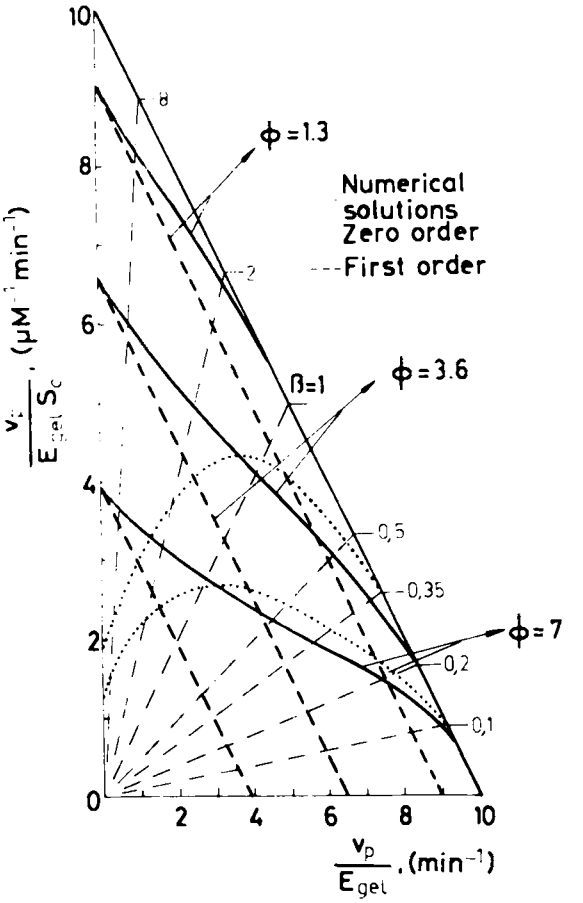

FIG. 1. Theoretical Eadie-Hofstee plots for three immobilized enzyme derivatives (solid lines). The line connecting values of 10 at the coordinates represents the behavior of a soluble enzyme obeying Michaelian kinetics. In the four cases values $k'_{cat} = 10$ min^{-1} and $K'_M = 1$ μM were considered. In the figure are also indicated the lines (. _ . _ . _) corresponding to values of β from 8 to 0.1.

portion of the curve ($\simeq -1/K'_M$). If values are now given to k'_{cat} we can calculate the values of $\emptyset$ and check the fit of the data to the theoretical model. The best fit will be achieved by testing several values of k'_{cat} and $\emptyset$.

Materials and Methods

Most items are described in the preceding paper (*1*). Sepharose 6B and CNBr-activated Sepharose 4B were Pharmacia products. CNBr activation of Sepharose 6B was carried out according to Porath et al. (*19*). Nuclease (EC. 3.1.4.7) was insolubilized on the CNBr-activated Sepharoses (4B and 6B) as previously reported (*20*).

The particle size was determined, before and after homogenization, using two different methods: direct observation in a microscope and conductimetry measurements in a Coulter apparatus (model Industrial D, Coulter Electronics

Ltd., Harpenden, England). The average radius, $\bar{R}$, was calculated by the equation

$$\bar{R} = (1/n)\ \Sigma_i\ R_i n_i$$

where n is the total number of particles examined, and n_i the number of particles whose radii fall in the interval represented by the values R_i. The average radius obtained was 50 μm before homogenization and 9 μm after homogenization.

Pore Radius

In the case of Sepharose 6B, Demassieux and Lachance (*21*) found by gel filtration an effective pore radius of 39 ± 1.68 nm, while Lasch et al. (*22*) obtained a value of 42 ± 3 nm by electron microscopy. From these figures we have assigned Sepharose 6B a pore radius of 40 nm.

Assuming that for globular proteins there is proportionality between their molecular weight and their effective molecular volume, employing equation

$$r_{p1}/r_{p2} = (\text{Exclusion limit}_1/\text{Exclusion limit}_2)^{1/3}$$

we can calculate the pore radius of Sepharoses 2B and 4B. Using exclusion limit values of 4×10^6, 20×10^6, and 40×10^6 daltons for Sepharoses 6B, 4B, and 2B, respectively (information from Pharmacia Fine Chemicals, Sweden), we obtain an approximate pore radius value of 68 nm for Sepharose 4B and of 86 nm for Sepharose 2B.

Table 1 lists some properties of the insolubilized enzyme derivatives used. A thorough study of the physical properties of the supports employed in this work will be the subject of a forthcoming paper.

Results

Diffusion Tests

As in the preceding paper (*1*), we verified, working under different conditions, that the reaction velocity was independent of the stirring speed. This external diffusion test has an important limitation: we must be sure that

TABLE 1
Properties of the Insolubilized Derivatives[a]

Support	$\bar{R}$, μm	r_p, nm	Derivative	E_{gel}, μM
Sepharose 2B	50	86	N-Se 2a	2.8
Sepharose 4B	50	68	N-Se 4a	2.8
Sepharose 6B	50	40	N-Se 6a	3.0
Sepharose 6B	9	40	N-Se $6a_{II}$	3.0
Sepharose 6B	50	40	N-Se 6b	0.93

[a] $\bar{R}$, mean radius; r_p, pore radius; E_{gel}, concentration of the insoluble enzyme in the gel.

when the stirring speed changes, u, the average velocity of the particles relative to the solvent also changes. As has been pointed out by Kasche et al. (*13*), u sometimes reaches a maximal value and then becomes independent of the stirring speed; in this case, varying the stirring speed does not alter the diffusional conditions, thus rendering the test incorrect. In our case this limitation of the test does not hold: if we assay the insoluble derivatives not with a small substrate but with high molecular weight substrates, we find a big change in reaction rate with the stirring speed (*23*). Therefore, we can be sure that in our conditions u varies with stirring speed.

With respect to internal diffusional limitations, there were, as we shall see below, conditions in which the diffusion was limiting and conditions in which it had no effect.

Effect of substrate concentration

The substrate concentration was varied between 3 and 200 μM. In this range, we studied how a change in the values of the kinetic constants affected the extent to which the internal diffusion limitations influenced the overall reaction rate. As in the preceding paper (*1*), we have investigated the effect of

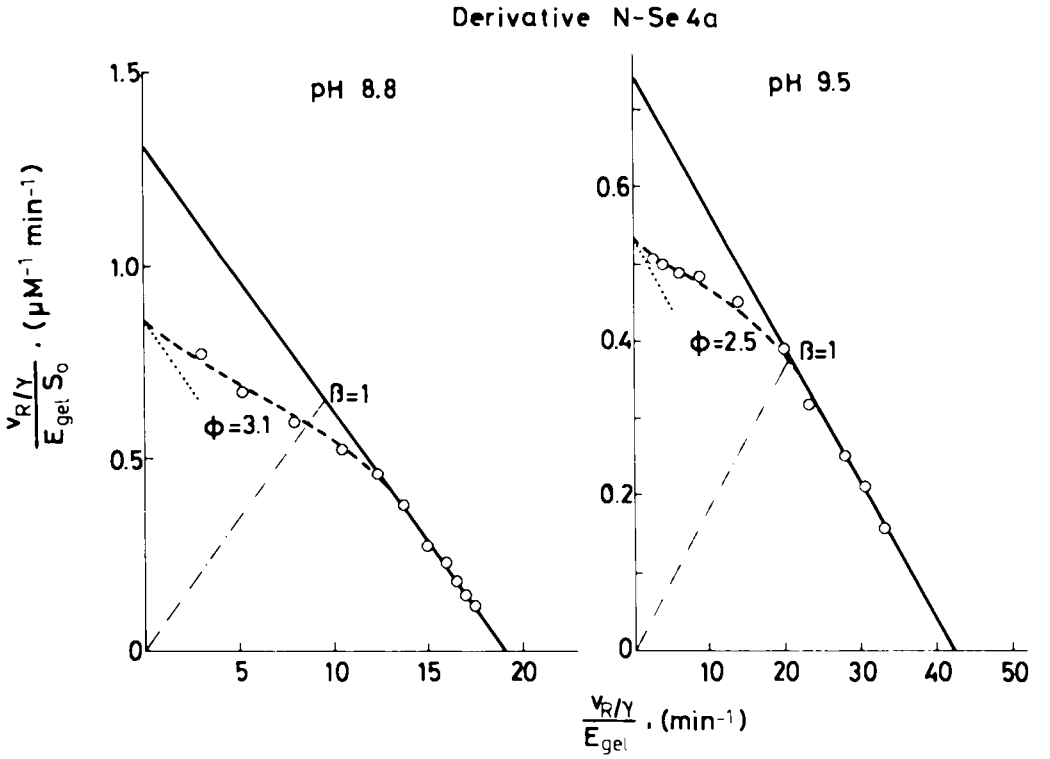

FIG. 2. Eadie-Hofstee plots for the N-Se 4a derivative (Table 1). Assay conditions: 25°C, 10 mM $CaCl_2$, and 25 mM Tris-HCl (pH 8.8) or 50 mM glycine-NaOH (pH 9.5) buffers. O, experimental results; —, Michaelian kinetics; . . . . ., first-order theoretical plots; - - - -, theoretical curves that fit the experimental data (the values obtained for the Thiele modulus are given in the graph).

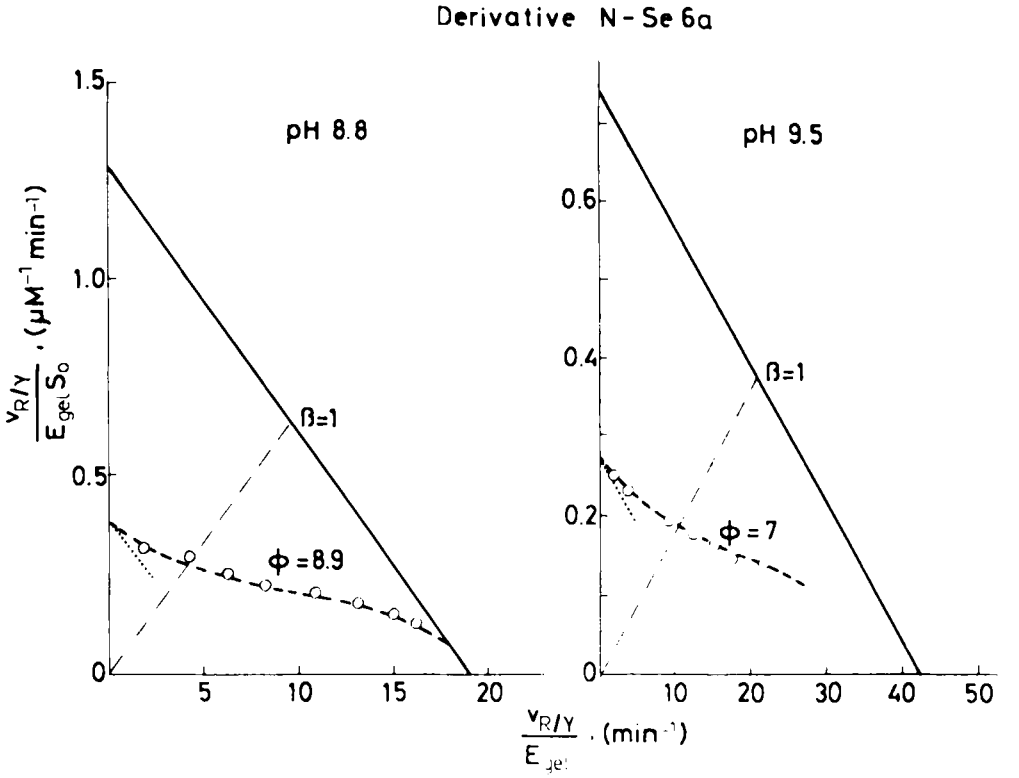

FIG. 3. Eadie-Hofstee plots for N-Se 6a derivative (Table 1). Other details as in Fig. 2.

substrate concentration under two different conditions: (a) 25 m*M* Tris-HCl buffer, 10 m*M* $CaCl_2$ (pH 8.8); (b) 50 m*M* glycine–NaOH buffer, 10 m*M* $CaCl_2$ (pH 9.5).

Figures 2 and 3 show the Eadie-Hofstee plots for derivatives N-Se 4a and N-Se 6a (see Table 1), respectively, in reaction conditions (a) and (b). Figure 4 depicts the behavior at pH 9.5 of derivatives N-Se 2a, N-Se 4a, and N-Se 6a; the enzyme concentration is similar in all three (see Table 1). Similarly, Fig. 5 compares the data found for derivatives based on Sepharose 6B as matrix: N-Se 6a, a derivative having less nuclease concentration (N-Se 6b) and another obtained using homogenized Sepharose 6B as support (N-Se $6a_H$). In all these figures, the broken lines represent the theoretical curve that best fits the experimental data; the values of ϕ obtained (by extrapolation) are also shown. Fitting was as described in the Theory section. The kinetics found with N-Se $6a_H$ fit almost perfectly to enzymic kinetics (type i), as was the case with derivatives prepared on Sepharose 2B (1). On the other hand, N-Se 6a follows internal diffusion kinetics (type ii), whereas derivatives N-Se 4a and N-Se 6b obey mixed internal diffusion–enzymic reaction kinetics (type iii).

If we carry out internal diffusion tests with the derivative N-Se 6a, we find that in all the conditions studied (at all the values of β and for both pHs) the reaction velocity is not proportional to enzyme concentration in the gel, and furthermore, diminishes when the particle radius increases. As an example,

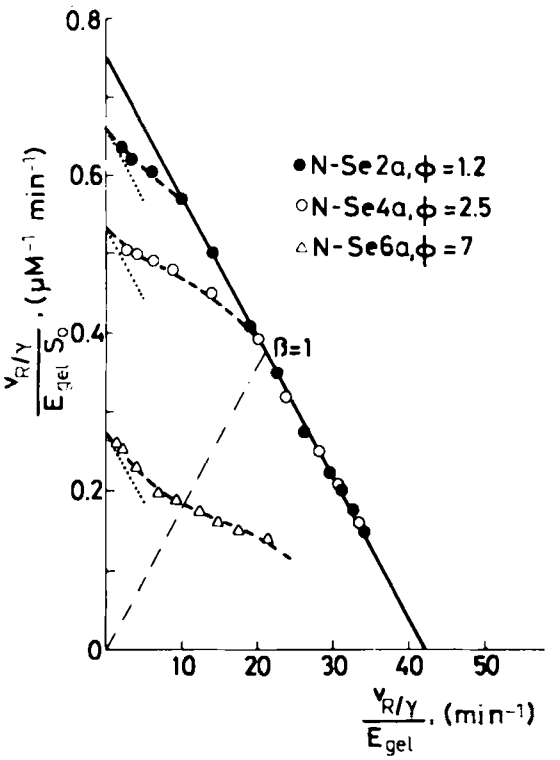

FIG. 4. Eadie-Hofstee plots for N-Se2a, N-Se4a and N-Se6a derivatives (Table 1) at pH 9.5. Other details as in Fig. 2. The data on N-Se2a are taken from the preceding paper (*1*).

Fig. 6 shows the values obtained at β values of 1 (graph A) and 0.35 (graph B). The theoretical model predicts that there are no diffusion restrictions for $\bar{R} < 9$ μm (graph A) and for $E_{gel} < 0.5$ μM (graph B). The experimental points fall on the curve defined by the model.

In the case of the other four derivatives, the presence or absence of diffusional restrictions depend on the β values (and, consequently, on S_o concentrations). In Figs. 2, 4, and 5 from the linear part of the graphs, that is, from the straight portion common to Michaelian kinetics, we obtain a single set of kinetic constants for derivatives N-Se 4a,N-Se 6b, and N-Se 6a$_H$:k'_{cat}, 19 min^{-1} at pH 8.8 and 42 min^{-1} at pH 9.5; K'_M, 14.7 μM at pH 8.8 and 56 μM at pH 9.5. These values are obviously the same as those found in the preceding paper for the derivatives having Sepharose 2B as support.

In the case of N-Se 6a, because of diffusion problems, it is not possible to obtain from the experimental points the values of k'_{cat} and K'_M. However, we have been able to get those values by homogenizing the Sepharose 6B beads or decreasing enzyme concentration in the support (cf., above paragraph). Knowing then k'_{cat} and K'_M indirectly we verified our model by following the above procedure when it was possible to obtain the values of the kinetic constants experimentally. The matching of theory and experimentation was very good.

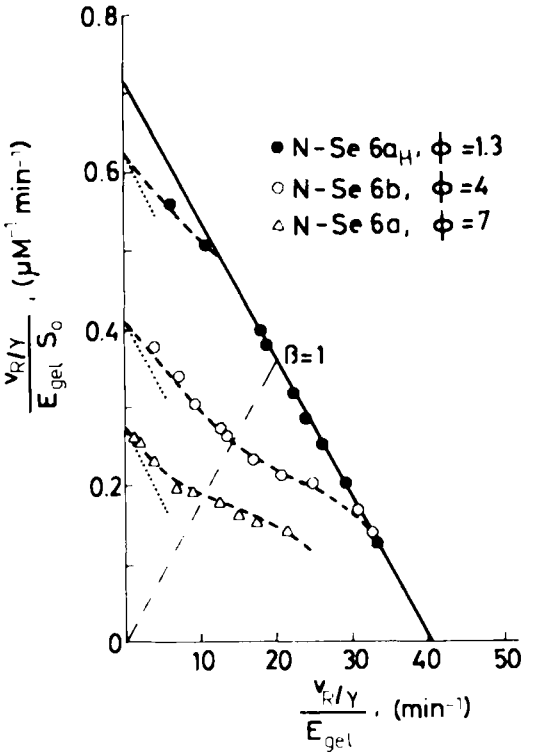

FIG. 5. Eadie-Hofstee plots for N-Se 6a$_H$, N-Se 6b, and N-Se 6a derivatives (Table 1) at pH 9.5. Other details as in Fig. 2.

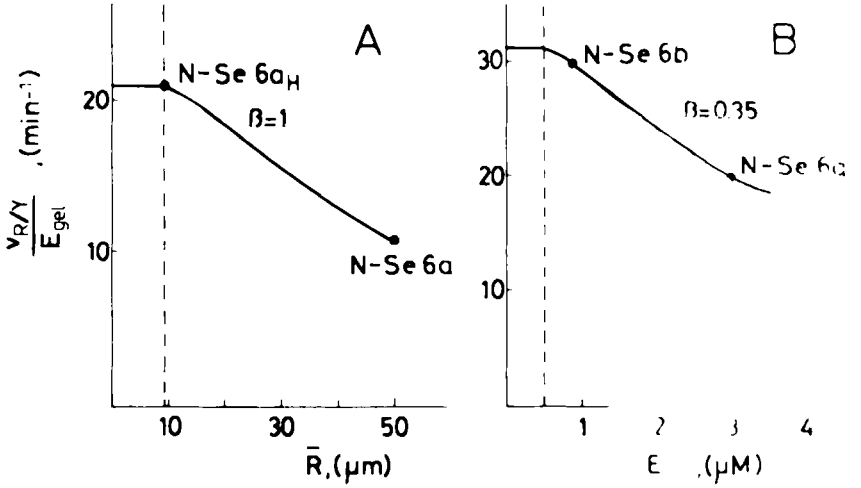

FIG. 6. Internal diffusion tests, pH 9.5, for derivatives N-Se 6a, N-Se 6a$_H$ and N-Se 6b (Table 1). k'_{cat} = 42 min^{-1}, K'_M = 56 μM, D_{eff} = 0.018 cm^2/s. (A) E_{gel} = 3 μM. (B) $\bar{R}$ = 50 μm. •, experimental results; —, theoretical curves (to the left of broken lines: absence of diffusional limitations; to the right: presence of diffusional limitations).

Once $\emptyset$ had been calculated according to the model, for several experimental conditions, and considering the definition of $\emptyset$, Eq. (2), we checked the numerical values of the following expressions

$$(a)\ \emptyset_1/\emptyset_2 = (k'_{cat1}\ K'_{M2}/k'_{cat2}\ K'_{M1})^{1/2} \tag{10}$$

$$(b)\ \emptyset_1/\emptyset_2 = R_1/R_2 \tag{11}$$

$$(c)\ \emptyset_1^{\infty}{}_{02} = (E_{gel1}/E_{gel2})^{1/2} \tag{12}$$

(assuming that in each case all the other variables are constant. In Tables 2 and 3 appear the values of the ratio $\emptyset_1/\emptyset_2$ (calculated), and in parenthesis the values (experimental) of the right-hand-side terms of expressions (a), (b), and (c). The close approximation of values demonstrates the usefulness of the proposed model in predicting the kinetic properties of these immobilized derivatives.

TABLE 2
Comparison of the Ratio of $\emptyset$ Values at pHs 9.5 and 8.89[a]

	$\emptyset$ (at 9.5)	
	Calculated	Experimental [Eq. (10)]
N-Se 2a	0.75	0.77
N-Se 4a	0.806	0.77
N-Se 6a	0.79	0.77

[a]Calculated and experimental values for derivatives N-Se 2a, N-Se 4a, and N-Se 6a.

TABLE 3
Comparison of the Calculated and Experimental Ratio of $\emptyset$ Values at pH 9.5, of Derivatives Obtained on Sepharose 6B as Support

$\emptyset$ (for N-Se 6a)/$\emptyset$ (for N-Se 6a$_H$)		$\emptyset$ (for N-Se 6a)/$\emptyset$ (for N-Se 6b)	
Calculated	Experimental [Eq. (11)]	Calculated	Experimental [Eq. (12)]
5.4	5.55	1.75	1.82

Discussion

Figures 2–5 show the fitting of the experimental results to the theoretical curves. In all cases there were values of $\emptyset$ that produced a very good fit. This is not surprising since the system is very simple and the *a priori* assumptions are warranted: (a) Support particles are spherical; (b) the absence of external diffusion restrictions was previously verified; (c) the model is based on Michaelian kinetics, which have been shown to apply in the case of the soluble enzyme (1, 24) and also in the case of other insoluble derivatives (*1*); and (d) the

assumption that the enzyme is uniformly distributed all over the particle has been qualitatively proven by fluorescence microscopy of derivatives prepared on Sepharose 4B as support (*25*).

At high concentrations of substrate we find the same kinetic behavior (i.e., the same values of k'_{cat} and K'_M) for all the derivatives unaffected by internal diffusion problems (N-Se 2a, N-Se 4a, N-Se $6a_H$, and N-Se 6b). To explain this coincidence we should consider that in all of them the support type is the same (the only difference being in the agarose concentration in the gel and in the resulting textural properties) and that the covalent bond(s) between enzyme and support is(are) also the same.

If, when studying immobilized enzyme systems, one finds that internal diffusion is limiting in all reaction conditions, one should proceed along the lines we have followed in this investigation: first, by decreasing the particle size or the concentration of enzyme immobilized per particle; the limitation must be eliminated in order to get the value of the kinetic constants. Second, if elimination is not possible experimentally, one should follow the fitting procedure outlined in the Theory section.

From the $\emptyset$ values obtained, we calculated, Eq. (2), the effective diffusion coefficients (D_{eff}) of the substrate in each of the insoluble derivatives. In Fig. 3, obviously, the values coincide for derivatives N-Se 6a, N-Se $6a_H$; and N-Se 6b. The value of the diffusion coefficient in solution, D_s, calculated by free substrate diffusion experiments, is 4×10^{-6} $cm^2 s^{-1}$ (manuscript in preparation). The values of D_s/D_{eff} (Table 4) are high, chiefly in the case of Sepharose 6B. These high values are consistent with the absence of external diffusion limitations: indeed the values of the apparent Sherwood number, Sh*, (equal to Sh $\times$ D_s/D_{eff}), must be very high, too (*13*). Lasch et al. (*22*), studying Sepharose 6B gels by electron microscopy, found that the inner space is a highly complicated network consisting of void spaces and spaces occupied by the matrix, not resembling any ideal pore pattern. This intricate structure could explain the fact that the diffusivity of substrate through the porous agarose network is very restricted, that is, high D_s/D_{eff} values were found.

In summary, we can say that under our experimental conditions, in which there is no influence of external diffusion, the kinetic behavior of insoluble Sepharose-(NH_2)nuclease derivatives fits very well the proposed theoretical model of mixed enzymic reaction–internal diffusion of the substrate kinetics.

TABLE 4
Parameter Values in the Insolubilized Derivatives

Derivative	η_1 (pH 9.5)	$\emptyset$ pH 9.5	$\emptyset$ pH 8.8	10^6 D_{eff}, cm^2 s^{-1}	D_s/D_{eff}
N-Se 2a	0.91	1.2	1.5	0.60	6.7
N-Se 4a	0.71	2.5	3.1	0.14	29
N-Se 6a	0.37	7.0	8.9	0.018	220
N-Se $6a_H$	0.90	1.3	1.7	0.019	210
N-Se 6b	0.55	4.0	—	0.018	220

Nomenclature

$S(r)$ Substrate concentration at distance r from particle center.
S_o Substrate concentration in bulk solution.
r Distance from particle center.
$\bar{R}$ Particle radius.
r_{pi} Mean pore radius.
E_{gel} Enzyme concentration in the immobilized derivative.
D_s Diffusion coefficient of substrate in solution.
D_{eff} Effective diffusion coefficient of substrate through porous network.
v_p Overall actual reaction rate per unit volume in an immobilized enzyme particle.
v_R Initial rate of product appearance per unit volume of the reactor.
K'_M Michaelis constant for immobilized enzyme.
k'_{cat} Catalytic constant for immobilized enzyme.
Y Dimensionless substrate concentration, $S(r)/S_o$.
ρ Dimensionless distance from particle center, r/R.
$\emptyset$ Thiele modulus, defined in Eq. (2).
β K'_M/S_o.
η Effectiveness factor, defined in Eq. (3).
η_o Effectiveness factor for a zero-order reaction.
η_1 Effectiveness factor for a first-order reaction.
ρ_e Value of ρ at which Y becomes zero.
γ Volume of immobilized enzyme derivative/volume of total reaction mixture.

Acknowledgments

We thank V. Kasche for stimulating comments, J. M. Engasser and V. Kasche for critical reading of the manuscript, and J. Serrano for help with some experiments and for helpful discussions. The expert technical assistance of M. C. Ceinos is also acknowledged. This research has been funded by the Spanish Comisión Asesora de Investigación Científica y Técnica.

References

1. Guisan, J. M., Melo, F. V., and Ballesteros, A. (1981), *Appl. Biochem. Biotechnol.* **6,** 000.
2. Kasche, V., Bergmann, R., Lundqvist, H. and Axen, R. (1971), *Biochem. Biophys. Res. Commun.* **45,** 615.
3. Engasser, J. M., and Horvath, C. (1973), *J. Theor. Biol.* **42,** 137.
4. March, D. R., Lee, Y. Y., and Tsao, G. T. (1973), *Biotechnol. Bioeng.* **15,** 483.
5. March, D. R. (1973), Kinetics of Glucoamylase Immobilized on Porous Glass, PhD. Thesis, Iowa State University, Ames.
6. Rovito, B. J., and Kittrell, J. R. (1973), *Biotechnol. Bioeng.* **15,** 143.
7. Horvath, C. and Engasser, J. M. (1974), *Biotechnol. Bioeng.* **16,** 909.

8. Kasche, V., and Bergwall, M. (1974), Intrinsic Molecular Properties and Inhibition of Immobilized Enzymes. Theory and Experimental Observations on α-Chymotrypsin: Sepharose, in *Insolubilized Enzymes*, Salmona, M., Saronio, C., and Garattini, S. (eds.), Raven, New York, pp. 77-86.
9. Korus, R., and O'Driscoll, K. F. (1974), *Can. J. Chem. Eng.* **52,** 775.
10. Regan, D. L., Lilly, M. D., and Dunnill, P. (1974), *Biotechnol. Bioeng.* **16,** 1081.
11. Buchholz, K., and Ruth, W. (1976), *Biotechnol. Bioeng.* **18,** 95.
12. Frouws, M. J., Vellenga, K., and De Wilt, H. G. J. (1976), *Biotechnol. Bioeng.* **18,** 53.
13. Kasche, V., Kapune, A., and Schwegler, H. (1979), *Enzyme Microb. Technol.* **1,** 41.
14. Franks, R. G. E. (1972), *Modeling and Simulation in Chemical Engineering*, Wiley, New York.
15. Weekman, V. W., and Gorring, R. L. (1965), *J. Catalysis* **4,** 260.
16. Wheeler, A. (1951), *Advan. Catalysis* **3,** 249.
17. Dowd, J. E., and Riggs, D. S. (1965), *J. Biol. Chem.* **240,** 863.
18. Engasser, J. M., and Horvath, C. (1976), Diffusion and Kinetics with Immobilized Enzymes, in *Applied Biochemistry and Bioengineering*, Vol. 1, Wingard, L. B., Jr., Katchalski-Katzir, E., and Goldstein, L. (eds.), Academic Press, New York, pp. 127-220.
19. Porath, J., Aspberg, K., Drevin, H., and Axen, R. (1973), *J. Chromatog.* **86,** 53.
20. Guisan, J. M., and Ballesteros, A. (1979), *J. Solid-Phase Biochem.* **4,** 245.
21. Demassieux, S., and Lachance, J. P. (1974), *J. Chromatog.* **89,** 251.
22. Lasch, J., Iwig, M., Koelsch, R., David, H., and Marx, I. (1975), *Eur. J. Biochem.* **60,** 163.
23. Guisan, J. M., and Ballesteros, A. (1981), *Enzyme Microb. Technol.*, in press.
24. Dunn, B. M., DiBello, C., and Anfinsen, C. B. (1973), *J. Biol. Chem.* **248,** 4769.
25. Guisan, J. M., Fernandez, V. M., and Ballesteros, A. (1980), Distribution on Staphylococcal Nuclease Insolubilized on Sepharose, in *Enzyme Engineering*, Vol. 5., Weetall, H. H., and Royer, G. P. (eds.), Plenum, New York, in press.